Chapter 2
LISA Data Processing Chain

Abstract The complete LISA data processing chain is described in this chapter, which consists of the simulation of the orbits, the simulation of gravitational wave signals, the simulation of various LISA measurements, the pre-processing stage, the time-delay interferometry techniques, and the astrophysical data analysis. The role and the goal of the pre-processing stage—first stage of LISA data analysis—is established and discussed for the first time.

2.1 Introduction

LISA (Laser Interferometer Space Antenna) [1, 2] is a proposed space-borne gravitational wave (GW) detector, aiming at various kinds of GW signals in the low frequency band between 0.1 mHz and 1 Hz. LISA consists of three identical spacecraft (S/C), each individually following a slightly elliptical orbit around the sun, trailing the Earth by about 20°. These orbits are chosen such that the three S/C retain, as much as possible, an equilateral triangular configuration with an arm length of about 5×10^9 m. This is accomplished by tilting the plane of the triangle by about 60° out of the ecliptic. Graphically, the triangular configuration makes a cartwheel motion around the Sun. As mentioned before, eLISA [3, 4] is a (evolving) variation of LISA, which consists of one mother S/C and two daughter S/C, separated from each other by 1×10^9 m. Although the configurations are slightly different, the principles and the techniques are equally applicable. Therefore, we will mainly focus on LISA hereafter.

Since GWs are propagating spacetime perturbations, they induce proper distance variations between test masses (TMs) [5], which are free-falling references inside the S/C shield. LISA measures GW signals by monitoring distance changes between the S/C. Spacetime is very stiff. Usually, even a fairly strong GW still produces only spacetime perturbations of order about 10^{-21} in dimensionless strain. This strain amplitude can introduce distance changes at the pm level in a 5×10^9 m arm length. Therefore, a capable GW detector must be able to monitor distance changes with this accuracy. The extremely precise measurements are supposed to be achieved by large laser interferometers. LISA makes use of heterodyne interferometers with coherent

Y. Wang, *First-stage LISA Data Processing and Gravitational Wave Data Analysis*,
Springer Theses, DOI 10.1007/978-3-319-26389-2_2

offset-phase locked transponders [6]. The phasemeter [7] measurements at each end are combined in postprocessing to form the equivalent of one or more Michelson interferometers. Information of proper-distance variations between TMs is contained in the phasemeter measurements.

Unlike the several existing ground-based interferometric GW detectors [8–12], the armlengths of LISA are varying significantly with time due to celestial mechanics in the solar system. As a result, the arm lengths are unequal by about 1 % (5×10^7 m), and the dominating laser frequency noise will not cancel out. The remaining laser frequency noise would be stronger than other noises by many orders of magnitude. Fortunately, the coupling between distance variations and the laser frequency noise is very well known and understood. Therefore, we can use time-delay interferometry (TDI) techniques [13–21], which combine the measurement data series with proper time delays, in order to cancel the laser frequency noise to the desired level.

However, the performance of TDI [18, 22] depends largely on the knowledge of armlengths and relative longitudinal velocities between the S/C, which are required to determine the correct delays to be adopted in the TDI combinations. In addition, the raw data are referred to the individual spacecraft clocks, which are not physically synchronized but independently drifting and jittering. This timing mismatch would degrade the performance of TDI variables. Therefore, they need to be referred to a virtual common "constellation clock" which needs to be synthesized from the inter-spacecraft measurements. Simultaneously, one also needs to extract the inter-spacecraft separations and synchronize the time-stamps properly to ensure the TDI performance.

2.2 Simulating the Whole LISA Data Processing Chain

In this section, I will talk about the perspective of a complete LISA simulation. The future goal is to simulate the entire LISA data processing chain as detailed as one can, so that one will be able to test the fidelity of the LISA data processing chain, verify the science potential of LISA and set requirements for the instruments. The flow chart of the whole simulation is shown in Fig. 2.1. In the following, I will discuss the role and the main task of each step.

2.2.1 LISA Orbits Simulator

The first step is to simulate LISA orbits under the solar system dynamics. It should provide the position and velocity of each TM, or roughly S/C, as functions of some nominal time, e.g. UTC (Coordinated universal time) for subsequent simulations. Since TDI requires knowledge of the delayed armlengths (or light travel times) to meter accuracies [23], and the pre data processing algorithms could hopefully determine the delayed armlengths to centimeter accuracies, the provided position

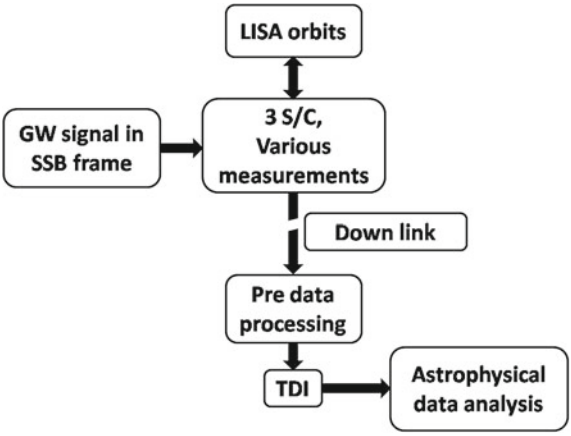

Fig. 2.1 LISA data processing chain

information should be more accurate than centimeters. Recall that 1 AU is of order 10^{11} m. The dynamic range here is 13 orders of magnitude, which is smaller than the machine accuracy (15–16 digits). However, the GW-induced arm-length variation for LISA is at the picometer level [23], which is 25 orders of magnitude smaller than 1 AU. One could in principle use extended precision, but that might be computationally too expensive. Luckily, GWs in the TT gauge do not change the coordinates of the TMs. Thus, one can ignore GWs when simulating LISA orbits.

One other issue is the sampling rate. The LISA onboard measurements will be down-sampled and transferred to the Earth at about Hz sampling rate (e.g. 3 Hz). So the position and velocity information should be provided to the centimeter precision at Hz sampling rate. In one year, there are about 10^8 samples at this sampling rate. One can design an orbit integrator with sub second integration time-steps, but it is inefficient. Instead, one can design an orbit integrator with adaptive large integration steps and then interpolate the orbits to centimeter precision. However, the accuracy of the interpolation scheme needs to be checked carefully.

The last issue in this step is to choose a model of dynamics. In principle, one should use the best known ephemeris (with trajectories of all the solar system planets) and the solar system dynamics to a sufficient PN order [24]. For simplicity and speed concern, sometimes one can also use Kepler orbits, or even simpler, analytical orbits (Taylor expansion of Kepler orbits to certain order of eccentricity) in the right place. One should make sure that it is consistent with all other steps.

2.2.2 Simulating GWs

The second step is to simulate GWs. There are various kinds of GW sources [23, 25] in the LISA band, such as massive black hole (MBH) binaries, extreme-mass-ratio inspirals (EMRIs), intermediate-mass-ratio inspirals (IMRIs), galactic

white dwarf binaries (WDBs), gravitational wave cosmic background etc. In the source frame, these GW waveforms are generated either from the dynamic equations or phenomenological waveform models. For some purposes, one can also simply use sinusoidal GW signals as test signals.

2.2.3 Simulating Measurements

The third step is to simulate the measurements as detailed as needed, which in turn requires the simulation of the evolution of the S/C internal environments, e.g. how does the attitude of TMs evolve, how does the frequency of the ultra-stable oscillator (USO) evolve, how does the temperature evolve, how does the laser frequency evolve? Since there are many sources of disturbance [26–28], one should first only take into account the critical ones. The less critical features can be ignored selectively. The irrelevant features should be ignored.

The TMs are drag-free in only one dimension each, which is along the direction of the laser beam. The other two transverse dimensions are controlled. Hence, their actual orbits may deviate from geodesics (i.e. orbits of three dimensional drag-free TMs). The deviation is small over short periods, but sizable after a few months accumulation.

Usually, these deviations are ignored in simulations. If one wants to simulate this effect, the orbits calculation and the measurements simulation must be integrated. Whenever the TMs tends to fall off the orbits, one should make corrections and calculate the new orbits. Mathematically, the equations of motion are augmented with the equations of the active control and the disturbances. The whole set of differential equations should be solved and evolved together.

There are many measurements in LISA. The main ones are science measurements, ranging measurements, clock side band beatnotes, S/C positions and clock offsets observed by the deep space network (DSN). There are many more measurements, such as various auxiliary measurements, incident beam angle measured by differential wavefront sensing (DWS). In principle, all the relevant measurements need to be simulated. The simulation in turn can guide the experiments and the design, telling us which measurements are useful and which ones need to be transferred back to the Earth at which sampling rate.

Another important issue is to simulate various kinds of noise sources, such as the laser-frequency noise, clock jitters, the readout noise, the acceleration noise. These noises are generated either from their PSD or from physical models. In the end, the noises and the GWs signals are both added to the measurements. For simplicity, usually stationary Gaussian noise (white or colored) is used, although real instruments in general produce more complicated noise.

2.2.4 Down Link

The 'down link' is referred to as a procedure of transferring the onboard measurement data back to Earth, which is also an important step in the simulation. Since the beat-notes between the incoming laser beam and the local laser are in the MHz range, the sampling rate of ADCs should be at least twice that, i.e. at least 40–50 MHz. The phasemeter prototype developed in the Albert Einstein Institute Hannover for ESA uses 80 MHz [29]. Due to the limited bandwidth of the down link to Earth, measurement data at this high sampling rate cannot be transferred to Earth. Instead, they are low-pass filtered and then down-sampled to a few Hz (e.g. 3 Hz). The raw data received on Earth are at this sampling rate.

For simulation concerns, generating measurement data at 80 MHz with a total observation time of a few years is computationally expensive and unnecessary. Instead, these measurements are simulated at a few tens to a few hundreds of Hz.

It is worth clarifying that, up to this point, the simulation of the S/C and GWs was done with complete knowledge of 'mother nature'. From the next subsection 'pre data processing' on, comes the the simulated processing of the down-linked data, where we have only the raw data received on Earth, but other informations such as the S/C status are unknown.

2.2.5 Pre Data Processing

The next step is the so-called pre data processing. The main task is to synchronize the raw data received at the Earth station and to determine the armlength accurately. In addition, pre data processing aims to establish a convenient framework to monitor the system performance, to compensate unexpected noise and to deal with unexpected cases such as when one laser link is broken for a short time.

The armlength information is contained in the ranging measurements, which compare the laser transmission time at the remote S/C and the reception time at the local S/C. Since these two times are measured by different clocks (or USOs), which have different unknown jitters and biases, the ranging data actually contain large biases. For instance, high-performance (not necessarily the best) space-qualified crystal oscillators, such as oven controlled crystal oscillators [30], have a frequency stability of about 10^{-7--8}. This would lead to clock biases larger than one second in three years, which would result in huge biases in the ranging measurements.

In fact, all the measurements taken in one S/C are labeled with the clock time in that S/C. This means all the time series contain clock noise. Time series from different S/C contain different clock noise. These unsynchronized, dirty and noisy time series need to be pre-processed in order to become usable for TDI.

Pre data processing has been ignored for long. It is one of the main topics of this thesis.

2.2.6 TDI Simulation

As mentioned previously, TDI has been well studied in the literature [14–21]. Laser frequency noise is the frequency instability of the laser source. For a normal Michelson interferometer, the laser beams travelling in the two arms originate from the same laser source, thus they share common laser frequency noise. At the photon detector, one measures the phase (or frequency) variation of the beatnote of the two laser beams. The frequency noise is canceled out when the two arms have the same length, hence not degrading the measurements.

However, in the LISA case, the S/C are far apart. The telescope can capture only a very small fraction of the remote laser beam, thus it is impossible to reflect the same laser light back to the remote S/C. The local photon detector measures the beatnote between the received weak laser beam and the local laser. Without the offset phase locking scheme, the two laser beams are generated by different laser sources, hence they contain different frequency noise. As a consequence, the laser frequency remains in the measurements. With the offset phase locking scheme [6], the laser frequency noise still remains, due to the unequal arm lengths. Its power spectral density is about 8–9 orders of magnitude higher than the designed sensitivity. Currently, the only solution is to phase-lock the remote laser, record each single-way measurement, properly recombine these single-way measurements in the TDI post-processing stage, virtually forming an equal-arm Michelson interferometer. In this step, one uses the ranging and the time information from pre data processing to properly shift the phasemeter measurements accordingly and recombine them.

2.2.7 Astrophysical Data Analysis

In this final step, the task is to dig out GW signals from the data and extract astrophysical information—in short, detection and parameter estimation. At this stage, we have relatively clean and synchronized data labeled with UTC time stamps. Still, the GW signals are weak compared to the remaining noise. As a result, one needs to implement matched filtering techniques to obtain optimal SNR. We will come to this again in detail in other chapters.

References

1. The LISA Study Team, Laser interferometer space antenna for the detection and observation of gravitational waves: Pre-phase a report. Max-Planck-Institute for quantum optics (1998)
2. K. Danzmann the LISA Study Team, LISA—an ESA cornerstone mission for the detection and observation of gravitational waves. Adv. Space Res. **32**, 12331242 (2003)
3. The Gravitational Universe, The eLISA constortium, Whitepaper submitted to ESA for the L2/L3 cosmic vision call. arXiv:1305.5720

4. P. Amaro-Seoane et al., eLISA: Astrophysics and cosmology in the millihertz regime. GW Notes **6**, 4–110 (2013). arXiv:1201.3621
5. L. Carbone et al., Achieving geodetic motion for lisa test masses: ground testing results. Phys. Rev. Lett. **91**, 151101 (2003)
6. P.W. McNamara, Weak-light phase locking for LISA. Class. Quantum Gravity **22**, S243–S247 (2005)
7. D. Shaddock, B. Ware, P. Halverson, R.E. Spero, B. Klipstein, Overview of the LISA phasemeter. 6th international LISA symposium, Greenbelt, Maryland, 19–23 June 2006
8. A. Abramovici et al., LIGO: the laser interferometer gravitational-wave observatory. Science **256**(5055), 325–333 (1992)
9. B.P. Abbott et al., LIGO: the laser interferometer gravitational-wave observatory. Rep. Prog. Phys. **72**, 076901 (2009)
10. B. Willke et al., The GEO 600 gravitational wave detector. Class. Quantum Gravity **19**, 1377 (2002)
11. B. Willke et al., The GEO-HF project. Class. Quantum Gravity **23**, S207 (2006)
12. B. Caron et al., The VIRGO interferometer for gravitational wave detection. Nucl. Phys. B, Proc. Suppl. **54**, 167 (1997)
13. G. de Vine, B. Ware, K. McKenzie, R.E. Spero, W.M. Klipstein, D.A. Shaddock, Experimental demonstration of time-delay interferometry for the laser interferometer space antenna. Phys. Rev. Lett. **104**, 211103 (2010)
14. T. Massimo, D. Shaddock, J. Sylvestre, J. Armstrong, Implementation of time-delay interferometry for LISA. Phys. Rev. D **67**, 122003 (2003)
15. J.W. Armstrong et al., Time-delay interferometry for space-based gravitational wave searches. ApJ **527**, 814–826 (1999)
16. N.J. Cornish, R.W. Hellings, The effects of orbital motion on LISA time delay interferometry. Class. Quantum Gravity **20**, 4851 (2003)
17. D.A. Shaddock, B. Ware, R.E. Spero, M. Vallisneri, Postprocessed time-delay interferometry for LISA. Phys. Rev. D **70**, 081101(R) (2004)
18. M. Vallisneri, Synthetic LISA: simulating time delay interferometry in a model LISA. Phys. Rev. D **71**, 022001 (2005)
19. T.A. Prince, M. Tinto, S.L. Larson, J.W. Armstrong, LISA optimal sensitivity. Phys. Rev. D **66**, 122002 (2002)
20. M. Tinto, S.V. Dhurandhar, Time-delay interferometry, Living Rev. Relativ. 8(4) (2005). arXiv:gr-qc/0409034. http://www.livingreviews.org/lrr-2005-4
21. M. Otto, G. Heinzel, K. Danzmann, TDI and clock noise removal for the split interferometry configuration of LISA. Class. Quantum Gravity **29**, 205003 (2012)
22. A. Petiteau et al., LISACode: a scientific simulator of LISA. Phys. Rev. D. **77**, 023002 (2008)
23. LISA International Science Team 2011, LISA assessment study report (Yellow Book) (European Space Agency) ESA/SRE(2011) 3. http://sci.esa.int/science-e/www/object/index.cfm?fobjectid=48364
24. E.M. Standish et al., Orbital ephemerides of the Sun, Moon, and Planets, in *Explanatory Supplement to the Astronomical Almanac*, ed. by P.K. Seidelmann (University Science Books, Mill Valley, 1992), pp. 279–323
25. S. Babak et al., Report on the second mock LISA data challenge. Class. Quantum Gravity **25**, 114037 (2008)
26. P.L. Bender, LISA sensitivity below 0.1 mHz. Class. Quantum Gravity **20**, S301–S310 (2003)
27. R.T. Stebbins et al., Current error estimates for LISA spurious accelerations. Class. Quantum Gravity **21**, S653–S660 (2004)
28. W.M. Folkner, F. Hechler, T.H. Sweetser, M.A. Vincent, P.L. Bender, LISA orbit selection and stability. Class. Quantum Gravity **14**, 1405–1410 (1997)
29. O. Gerberding et al., Phasemeter core for intersatellite laser heterodyne interferometry: modelling, simulations and experiments. Class. Quantum Gravity **30**(235029), 16 (2013)
30. Space oven controlled crystal oscillator. http://www.q-tech.com/assets/datasheets/spaceOCXO.pdf

http://www.springer.com/978-3-319-26388-5

First-stage LISA Data Processing and Gravitational Wave Data Analysis
Ultraprecise Inter-satellite Laser Ranging, Clock Synchronization and Novel Gravitational Wave Data Analysis Algorithms
Wang, Y.
2016, XXX, 228 p. 97 illus., 1 illus. in color., Hardcover
ISBN: 978-3-319-26388-5